Catalysis Today 141 (2009) 89–93

Contents lists available at ScienceDirect

Catalysis Today

journal homepage: www.elsevier.com/locate/cattod

Ce (III) species supported zeolites as novel photocatalysts for hydrogen production from water

J. Krishna Reddy, G. Suresh, C.H. Hymavathi, V. Durga Kumari *, M. Subrahmanyam

Inorganic and Physical Chemistry Division, Indian Institute of Chemical Technology, Hyderabad 500607, India

ARTICLE INFO

Article history:
Available online 27 June 2008

Keywords:
Cerium
Zeolite support
Photocatalysts
Water splitting

ABSTRACT

Cerium (0.3–3.2 wt.%) modified MCM-41, Al-MCM-41, HZSM-5 and HY systems were prepared by impregnation method. These catalysts were characterized by XRD, DRS and XPS techniques. DRS clearly shows a blue shift of 50 nm in the absorption edge of CeO_2 at low loadings of Ce on zeolites indicating the size quantization and high dispersion of cerium particles. XPS analyses of samples containing low cerium content revealed the existence of strong interaction between zeolites and cerium wherein most of the cerium is in Ce^{3+} state. Photoactivity of these Ce-modified zeolite catalysts was evaluated in the photogeneration of hydrogen from water under UV irradiation. Among the catalysts prepared Ce-MCM-41 was found to be a promising photocatalyst for hydrogen production from water.

1. Introduction

In recent years semiconductor oxide photocatalysis is gaining importance in the conversion of photon energy into chemical energy [1,2]. Much attention has been paid to the photocatalytic decomposition of water into H_2 and O_2 over semiconductor materials, as it can potentially provide a clean and renewable source for hydrogen fuel in the future. Variety of photocatalysts mainly Ti [3–5], Nb [6,7] and Ta-based [8–14] oxides have been reported to be effective for the photocatalytic decomposition of water.

On the other hand rare earth oxides have been widely investigated for several applications such as lasers, optical amplifiers, light emitting diodes, etc. [15,16]. They are also known for their potential abilities to induce photocatalytic reactions by absorbing light via 'f–d' or 'f–f' orbital transitions [17]. Ceria is the most abundant rare earth oxide with good redox properties and acquired much importance as an electron acceptor or sacrificial agent in aqueous photoelectrochemical reactions since it can oxidize and reduce reversibly at (E° of $Ce^{3+}/Ce^{4+} = +1.44$ V) [18]. Few studies on ceriumdioxide as a water splitting photocatalyst are reported [18,19]. However, the photocatalytic reactions of cerium (Ce^{3+}/Ce^{4+}) by the redox couple is not widely explored. Therefore in the present investigation an attempt has been made to stabilize Ce ion by interacting with a zeolite support and understanding the chemistry of the redox couple in the photodecomposition of water.

2. Experimental

2.1. Chemicals and materials

Tetra ethyl ortho silicate (TEOS), cetyl trimethyl ammonium bromide (CTAB) and aluminium isopropoxide are from Aldrich chemicals. Cerium (III) nitrate was obtained from Loba Chemie (India) and sodium hydroxide is from S.D. Fine Chemicals. HY and HZSM-5 zeolites are from PQ corporation (USA), Conteka (Sweden) with Si/Al ratio = 2.6 and 15, respectively.

2.2. Preparation of MCM-41 and Al-MCM-41

MCM-41 and Al-MCM-41 mesoporous materials were prepared according to the reported procedure [20]. An aqueous solution of sodium hydroxide (0.3 g) is added to 9.3 g of tetra ethyl ammonium hydroxide (TEAOH) while cooling under stirring (solution A). Simultaneously 25 g of tetraethyl ortho silicate was taken in another beaker in 50 ml water (solution B) and then solution A was slowly added to solution B while stirring. 10.55 g of cetyl trimethyl ammonium bromide (CTAB) was added slowly to the above mixture. Finally the gel mixture with molar composition SiO_2:0.23CTAB:0.3TEAOH:0.26Na_2O:125H_2O was transferred to an autoclave and heated at 100 °C for 24 h. The recovered product was calcined at 500 °C in air for 12 h to expel the imprisoned template. Aluminium isopropoxide is added to solution A to obtain Al-MCM-41 with Si/Al ratio of 15.5.

---

* Corresponding author. Tel.: +91 40 27193165; fax: +91 40 27160921.
E-mail address: durgakumari@iict.res.in (V. Durga Kumari).

0920-5861/$ – see front matter © 2008 Published by Elsevier B.V.
doi:10.1016/j.cattod.2008.05.012

2.3. Preparation of cerium-modified catalysts

Cerium-modified MCM-41, Al-MCM-41, HY and H-ZSM-5 were prepared by impregnation of cerium nitrate salt dissolved in minimum quantity of distilled water to which a known quantity of zeolite support was added and dried in oven at 100 °C over night followed by calcination at 450 °C for 5 h.

2.4. Catalyst characterization

Powder XRD patterns were recorded with a Siemens D-5000 X-ray diffractometer using Cu Kα radiation. UV–vis DR spectra were recorded on Cintra 10e spectrometer using pellets of 50 mg sample ground with 2.5 g of KBr. XPS were recorded on a KRATOS AXIS 165 photoelectron spectroscopy using the Mg Kα radiation (150 W) anode taking C 1s level as an internal standard.

2.5. Photocatalytic experiments

The photocatalytic reactions were carried out in a gas-closed circulation system. A catalyst sample of 0.05 g was dispersed in 50 ml of solution in a quartz reactor (100 cm^3) and illuminated with 400 W Hg vapor lamp. Prior to start of light experiments dark experiments were carried out for 30 min under continuous stirring. The evolved H_2 and O_2 gases were analyzed using molecular sieve-5A column in gas chromatograph (Shimadzu GC 8A) with thermal conductivity detector.

3. Results and discussion

3.1. XRD

Powder X-ray diffractograms of MCM-41, Al-MCM-41, Ce-MCM-41, Ce–Al-MCM-41, Ce-ZSM-5 and Ce–Y are shown in Fig. 1. Prominent high intensity peaks (1 0 0) in the range of 1.5–2.0 θ° and less intense peaks (1 1 0), (2 0 0), (2 1 0) in the range $2\theta < 5$ observed are the characteristics of MCM-41 and Al-MCM-41 [21]. On dispersing cerium ion slight decrease in the intensity of the characteristic (1 0 0) peak is observed. No characteristic peaks of crystalline CeO_2 phase ($2\theta > 25$) are observed even at 3 wt.% of cerium loadings which indicates that metal ions are either interacted with the support or dispersed on the surface of the mesopore. The XRD patterns of Ce-ZSM-5 and Ce–Y show only the characteristic peaks of parent H-ZSM-5 and HY zeolite.

3.2. UV–vis DRS

The diffuse reflectance spectroscopy (DRS) is known to be a very sensitive technique for the identification of absorption band of metal ions. The DRS of CeO_2 and cerium dispersed over zeolite supports are shown in Fig. 2. The bare ceria shows a large absorption band around 370 nm (Fig. 2 IV) due to the charge transfer from O (valence band) to Ce (conduction band) [17]. On incorporating small amount of cerium on the zeolite support a band around 290–300 nm is observed in all the Ce-supported zeolites. Large blue shift in the absorption edge of ceria at low

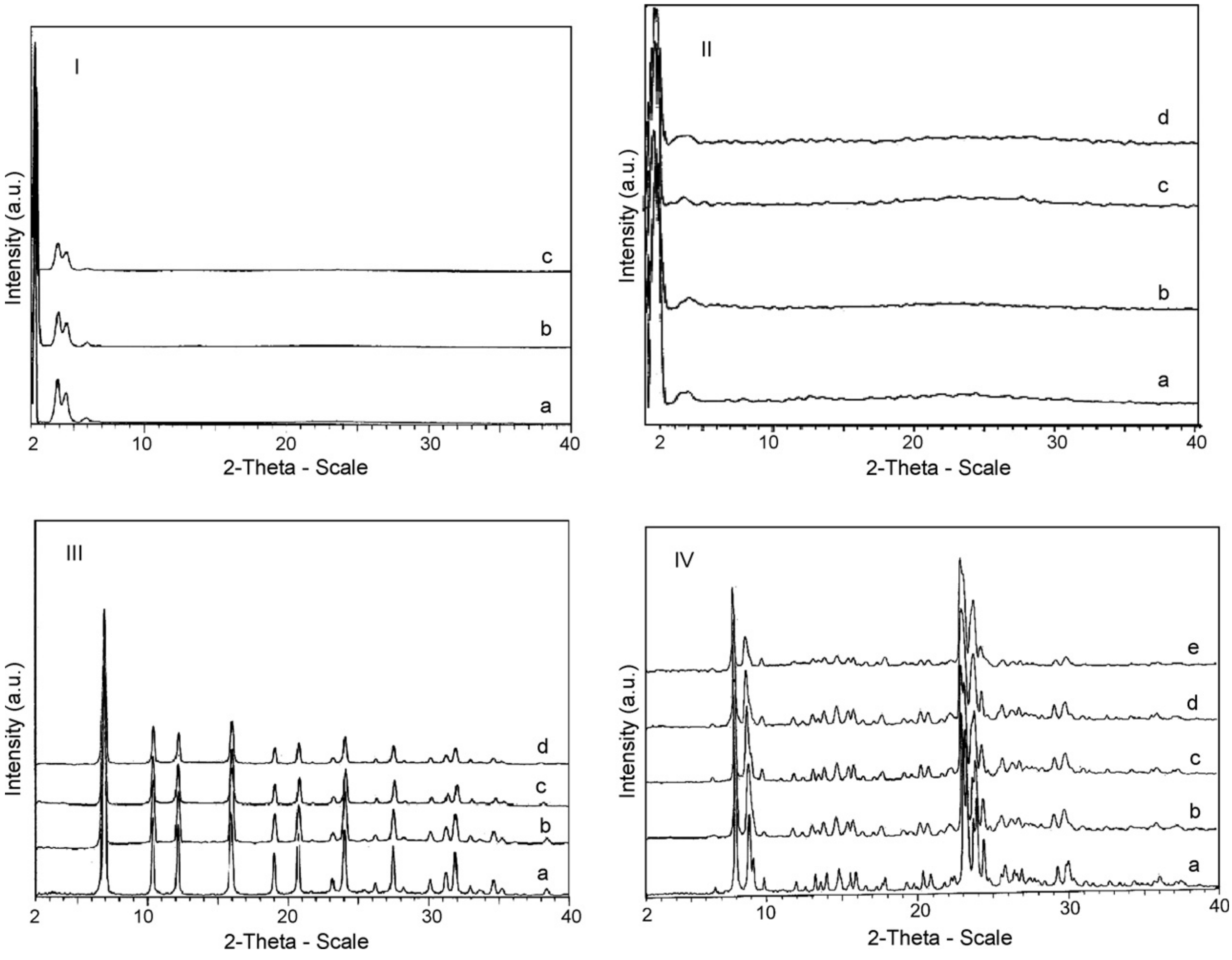

Fig. 1. XRD patterns of cerium (wt.%) modified: (a) 0, (b) 0.3, (c) 0.8, (d) 1.6, and (e) 2.4 I (MCM-41), II (Al-MCM-41), III (HY) and IV (HZSM-5) supports.

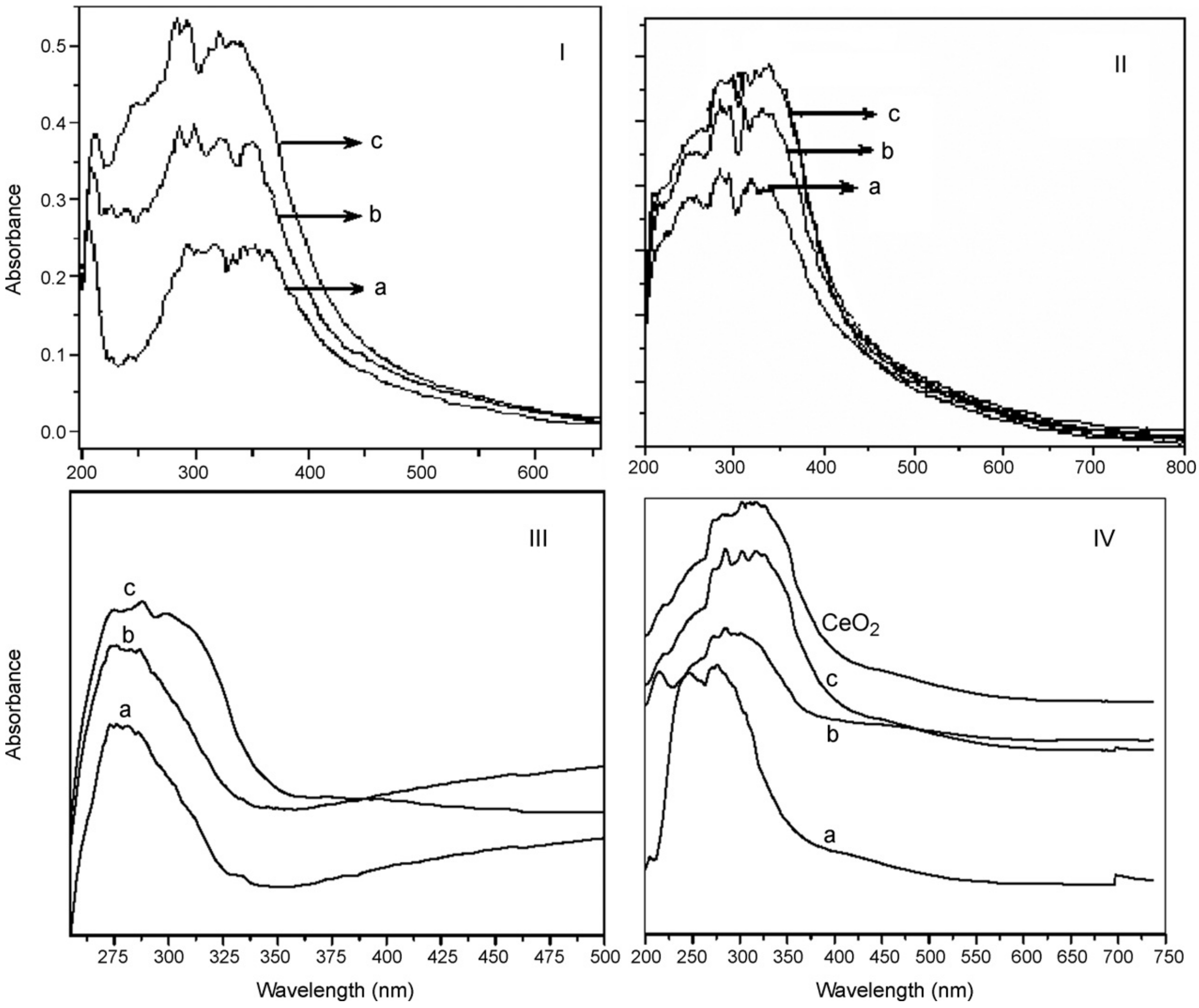

Fig. 2. UV–vis DRS of cerium (wt.%): (a) 0.3, (b) 0.8, and (c) 1.6 modified I (HY), II (HZSM-5), III (MCM-41), IV (Al-MCM-41) and CeO_2.

loadings may be seen due to interaction of cerium ion with the support [22]. Earlier reports on dispersion of ceria at low loadings confirmed that the bands around 300 nm are due to 4f–5d transition of the Ce^{3+} ion [17,23]. Further more with increase of cerium loading, this band is shifted towards that of pure ceria (370 nm). Variation of the band edge shown at different cerium loadings is due to size quantization effect [24]. From the DRS results it is clear that the chemical environment of cerium at low loadings is different from that of samples with high loadings.

3.3. XPS

The XPS analysis of CeO_2, Ce modified MCM-41 and Al-MCM-41 catalysts are shown in Fig. 3. The peaks appeared between 880 and 895 eV correspond to Ce $3d_{5/2}$ and 895–910 eV to Ce $3d_{3/2}$. The peak at 916 eV is a characteristic feature of Ce^{4+} [25]. In general eight distinct peaks are observed in the spectra of pure ceria due to +3 and +4 oxidation states of cerium. The peaks attributed to Ce^{3+} and Ce^{4+} in Fig. 3 are clearly distinguishable as reported earlier [26]. MCM-41 and Al-MCM-41 modified with low Ce (0.3 wt.%) content show high intense peaks at 885.9 and 904.2 eV corresponding to Ce^{3+} (Fig. 3A). No characteristic peaks of Ce^{4+} are observed on these samples indicating that Ce exists in +3 oxidation sate. For pure ceria and high (0.8 and 3.0 wt.%) Ce loaded samples, the high intense peaks observed at 882.2 and 898.4 eV are due to Ce^{4+} which is strongly supported by the presence of another characteristic peak at 916 eV (Fig. 3B). The XPS analysis of ceria and high Ce loaded samples also show the peaks corresponding to Ce^{3+} indicating that Ce exists both in +3 and +4 oxidation states in these samples and as the Ce content increases the intensity of characteristic Ce^{4+} peak tends to increase as shown in Fig. 3B. From these results it is understood that when cerium is impregnated in small amounts on zeolite supports, the particles are highly dispersed and interacted with the support wherein most of the cerium is in +3 oxidation state.

3.4. Photocatalytic activity

3.4.1. Effect of cerium loading on zeolites

The activity studies of cerium (0.3–3.2 wt.%) modified zeolite systems for water splitting under UV irradiation are shown in Table 1. The Ce-modified catalysts are showing enhanced photocatalytic activity compared to bare CeO_2. The optimum loading of cerium content on different supports is varied from 0.3 to 1.6 wt.% and the activity order, $CeO_2 < 0.8$ wt.%Ce–Y < 1.6 wt.%Ce-ZSM-5 < 0.3 wt.%Ce–Al-MCM-41 < 0.3 wt.% Ce-MCM-41 in terms of H_2 production rates is shown in Fig. 4. Ce-modified MCM-41 and Al-MCM-41 are showing H_2 and O_2 evolution close to the stoichiometry. Whereas Ce-modified HY and HZSM-5 are showing high O_2 evolution deviating from the stoichiometry. The basic

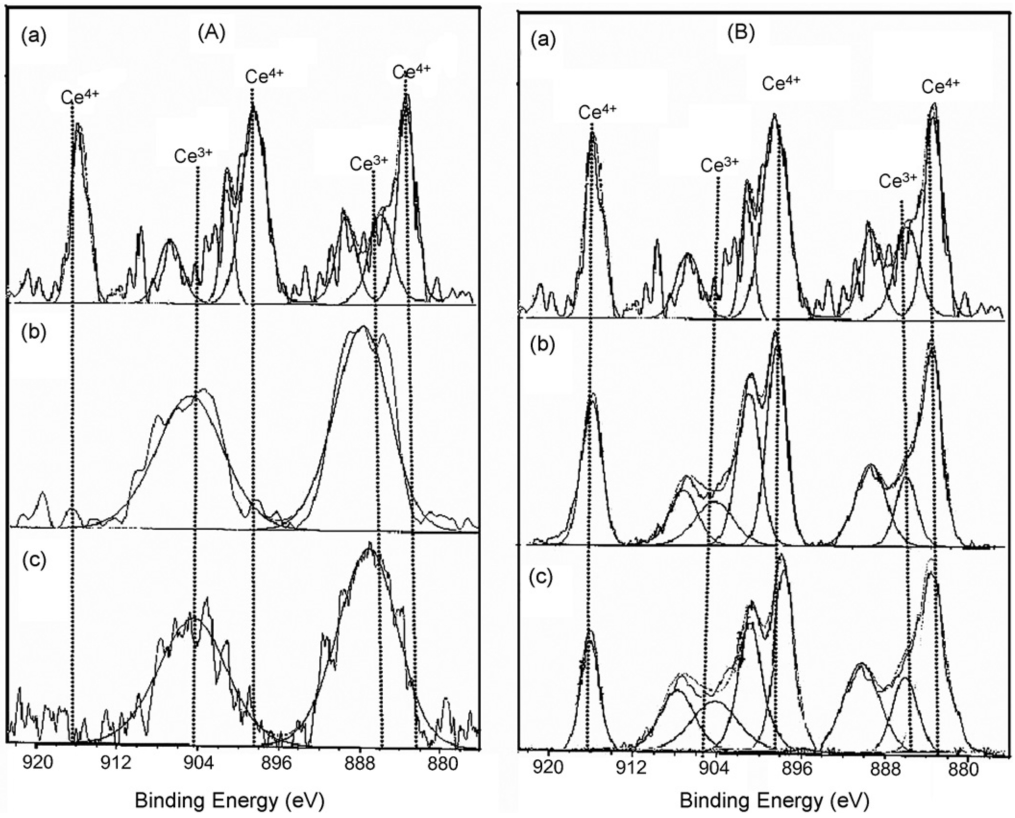

Fig. 3. (A) XPS of (a) ceria, 0.3 wt.% Ce modified (b) MCM-41 and (c) Al-MCM-41. (B) XPS of (a) ceria, (b) 3.0 and (c) 0.8 wt.% modified Al-MCM-41.

requirements for the reactions of photocatalytic water splitting are that the potential on the bottom of the conduction band should be above the reduction potential of H^+/H_2, and the potential on the top of the valence band should be below the oxidation potential of O_2/H_2O. Furthermore, if the conduction band potential is more negative compared to reduction potential of H^+/H_2 the rate of H_2 evolution will be more. Our results clearly indicate that the overall photo cleavage of water was thermodynamically feasible on Ce modified zeolites as listed in Table 1 Further the rate of H_2 evolution is also seen governed by surface area, porosity and Si/Al ratio of the zeolites.

3.4.2. Effect of surface area, porosity and Si/Al ratio of the zeolites

HY and HZSM-5 are the microporous zeolites whereas MCM-41 and Al-MCM-41 are mesoporous materials. Better activity is observed on mesoporous materials compared to HY and HZSM-5. This may be seen as due to large pore and high surface area of the mesoporous materials. In MCM-41 and Al-MCM-41 cerium in lower amounts is highly dispersed and strongly interacted with the walls of the mesopore.

With an increase in aluminium content the order of activity is Ce-MCM-41 (Al = 0) > Ce–Al-MCM-41(Si/Al = 15.5) > Ce-ZSM-5 (Si/Al = 15) > Ce–Y (Si/Al = 2.75). Ce-modified MCM-41 with

Table 1
Photocatalytic activity of cerium supported zeolite catalysts

Support	Ce (wt.%)	H_2 (μmol/(h gm l)	O_2 (μmol/(h gm l)
MCM-41	0.0	0.0	0.0
	0.3	1416	305
	0.8	116	35
Al-MCM-41	0.0	0.0	0.0
	0.3	651	420
	0.8	94.5	60
HZSM-5	0.0	0.0	0.0
	0.3	29	1713
	0.8	49	213
	1.6	231	788
	2.4	116	1373
	3.2	25	798
HY	0.0	0.0	0.0
	0.3	23	421
	0.8	121	242
	1.6	67	1682
	2	58	896
CeO_2	–	0.25	355

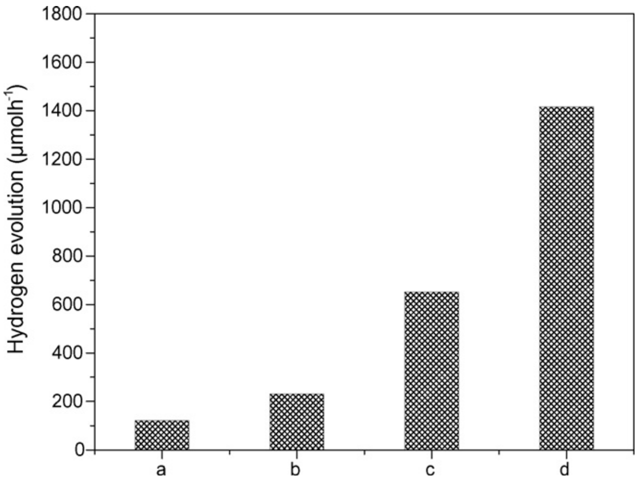

Fig. 4. Comparison of hydrogen evolution activity on optimized Ce-modified catalysts: (a) 0.8 wt.% Ce–Y, (b) 1.6 wt.% Ce-ZSM-5, (c) 0.3 wt.% Ce-Al-MCM-41, and (d) 0.3 wt.% MCM-41 supports.

out Al showed maximum photocatalytic-activity. The very presence of Al in the zeolites is responsible for both Lewis and Bronstead acidity. Al with its Lewis acidity traps the excited electron resulting in decreased photoactivity of the catalyst which in turn decreases the photogeneration of H_2 during water splitting. Therefore, it is understood that the zeolite supports with out Al content are more suitable for the effective photocatalytic water splitting.

3.4.3. Redox chemistry of Ce (Ce^{3+}/Ce^{4+}) in photocatalytic water splitting

Based on the above observations we propose a mechanism wherein Ce^{3+} is directly excited by UV light releasing an electron (step-1). Thus released electron is captured by the water molecule and gives H_2 gas (step-2). The hydroxide ion formed is trapped by Ce^{4+} ion resulting Ce^{3+} ion and OH radical (step-3) that finally leads to the generation of O_2 (step-4). The proposed mechanism is in agreement with the reported literature [27–30]:

$$Ce^{3+} \xrightarrow{h\nu} Ce^{4+} + e^- \tag{1}$$

$$2H_2O + 2e^- \rightarrow H_2\uparrow + 2OH^- \tag{2}$$

$$Ce^{4+} + OH^- \rightarrow Ce^{3+} + {}^{\bullet}OH \tag{3}$$

$${}^{\bullet}OH + {}^{\bullet}OH \rightarrow H_2O + 1/2\,O_2\uparrow \tag{4}$$

4. Conclusions

The surface modification of zeolites with cerium is showing higher photocatalytic water splitting activity compared to bare ceria. At lower Ce loadings it interacts with support and exists as Ce^{3+} species. The photoirradiation of Ce^{3+} species generates electrons ($Ce^{3+} + h\nu \rightarrow Ce^{4+} + e^-$) that are captured effectively by water molecule for the production of hydrogen.

Acknowledgement

The authors thank MNRE, New Delhi for the financial support.

References

[1] M.A. Fox, M.T. Dulay, Chem. Rev. 93 (1993) 341.
[2] A. Fujishima, T.N. Rao, D.A. Tryk, J. Photochem. Photobiol. Photochem. Rev. 1 (2000) 1.
[3] K. Domen, S. Naito, T. Onishi, K. Tamaru, Chem. Phys. Lett. 92 (1982) 433.
[4] Y. Inoue, T. Kubokawa, K. Sato, Chem. Commun. (1990) 1298.
[5] T. Takata, Y. Furumi, K. Shinohara, A. Tanaka, M. Hara, J.N. Kondo, K. Domen, Chem. Mater. 9 (1997) 1063.
[6] A. Kudo, K. Sayama, A. Tanaka, K. Asakura, K. Domen, K. Maruya, T. Onishi, J. Catal. 120 (1989) 337.
[7] K. Sayama, A. Tanaka, K. Domen, K. Maruya, T. Onishi, J. Phys. Chem. 95 (1991) 1345.
[8] A. Kudo, H. Kato, Chem. Lett. (1997) 867.
[9] T. Ishihara, H. Nishiguchi, K. Fukamachi, Y. Takita, J. Phys. Chem. B 1 (1999) 103.
[10] A. Kudo, H. Kato, S. Nakagawa, J. Phys. Chem. B 104 (2000) 571.
[11] H. Kato, A. Kudo, J. Phys. Chem. B 105 (2001) 4285.
[12] A. Kudo, K. Asakura, H. Kato, J. Am. Chem. Soc. 125 (2003) 3082.
[13] Z. Zou, J. Ye, K. Sayama, H. Arakawa, Nature 414 (2001) 625.
[14] M. Machida, J. Yabunaka, T. Kijima, Chem. Mater. 12 (2000) 812.
[15] J.L. Adam, Chem. Rev. 102 (2002) 2461.
[16] M. Sopinsky, V. Khomchenko, Curr. Opin. Solid State Mater. Sci. 7 (2003) 97.
[17] L. Yuliati, T. Hamajima, T. Hattori, H. Yoshida, Chem. Commun. (2005) 4824.
[18] G.R. Bamwenda, H. Arakawa, J. Mol. Catal. A 161 (2000) 105.
[19] K.H. Chug, D.C. Park, Catal. Today 30 (1996) 157.
[20] A. Ratnamala, V. Durga Kumari, K. Lalitha, M. Subrahmanyam, Catal. Commun. 8 (2007) 267.
[21] M.D. Kadgaonkar, S.C. Laha, R.K. Pandey, P. Kumar, S.P. Mirajkar, R. Kumar, Catal. Today 97 (2004) 225.
[22] S. Damyanova, C.A. Perez, M. Schmal, J.M.C. Bueno, Appl. Catal. B 234 (2002) 271.
[23] G.K. DasMohapatra, Mater. Lett. 35 (1998) 120.
[24] A. Bensalem, F.B. Verduraz, M. Delamar, G. Bugli, Appl. Catal. A 121 (1995) 81.
[25] C. Korsvik, S. Patil, S. Seal, W.T. Self, Chem. Commun. (2007) 1056.
[26] I. Avramova, P. Stefanov, D. Nicolova, D. Stoychev, T. Marinova, Compos. Sci. Technol. 65 (2005) 1663.
[27] M.G. Evans, N. Uri, Nature 66 (1950) 602.
[28] G.D. Andel, J.M. Padilla, I. Cuauhtemoc, J. Navarrete, J. Mol. Catal. A 281 (2008) 173.
[29] K. Thampi, M. Gratzel, J. Mol. Catal. A 60 (1990) 31.
[30] G.R. Bamwenda, H. Arakawa, Appl. Catal. A 210 (2001) 181.